The impact of the JWST Point Spread Function on the recoverability of the structural parameters of faint galaxies: a critical comparison of six proposed mirror configurations

Rolf A. Jansen & Rogier A. Windhorst

Dept. of Physics & Astronomy, Arizona State University, P.O. Box 871504, Tempe AZ 85287; `Rolf.Jansen` *or* `Rogier.Windhorst@asu.edu`

ABSTRACT

We present the preliminary results of a set of simulations designed to evaluate the impact of the JWST Point Spread Function (PSF) on the accuracy with which structural parameters may be recovered for faint galaxies and sub-galactic objects at high redshifts $3 \lesssim z \lesssim 20$. In a previous study we used simple approximations for the JWST PSF and simulated source fields to evaluate the impact of a non-circular primary aperture. Here, we use the actual PSF's as computed by Ball Aerospace for the different designs for the segmented primary mirror assembly under study and the Hubble Deep Field North as source field.

We evaluate the impact of (1) aperture size for identical JWST mirror configurations, (2) mirror configuration for identical clear apertures, (3) type of mirror actuation and control, and (4) aperture shape. We will focus on the short wavelength channel of NIRCAM at 0.7μm, because the impact of the choice of mirror design will be largest at wavelengths shortward of 2.0μm.

Our main results are, that: (1) To first order, the differences between the various round PSF's and their impact on faint galaxy parameter determination, are realtively small; (2) but the hexapod mirror actuation recovers object structural parameters better than tip/tilt/piston actuation at 0.7μm; and (3) a noticeable increase in overall noise is seen when going from a 7.0 to a 6.5 m telescope.

1. Introduction

Ball PSF's were available at 0.7 and 2.0 micron, and simulations were started at 0.7 micron to monitor the behavior of JWST's short wavelength PSF (the one that stands to loose the most during the various descopes).

More intro... here

2. Primary mirror configuration

Presently, there are two distinct configurations for the primary mirror assembly under study. Both configurations are build using hexagonal segments. The first configuration (essentially as in the original TRW proposal) consists of 36 such segments and results in a primary mirror diameter of either 6.5 m (descope option 3) or 6.2 m (option 1B), while the second configuration uses 18, larger, segments for a diameter of either 6.6 m (option 4) or 6.3 m (option 2B) (see Fig. 1 and Tab. 1). For each configuration, both a tip/tilt/piston (3 degrees of freedom [DoF]) and a hexapod (6 DoF) mirror support and actuation are considered.

It is worth noting that all proposed descope options represent a larger descope with respect to the original requirements and original configuration proposed by TRW than one might expect, both in terms of total surface area and in terms of resolution. For instance, for the 6.5 m mirror diameter quoted for descope option 3, one might expect a total surface area of $A = \pi * 3.25^2 \simeq 33.2$ m^2, giving a total clear aperture (after correction for the central hole and obscuration by the tripod support structure of the secondary) of $A_{\rm clear} = 30$ m^2. For the angular resolution at 2.0μm one would expect FWHM $= 2\,\theta_1 = 2 \cdot 1.22 \cdot (\lambda/D) = 0''.155$. Neither of these expectations are met by the actual mirror. This is because the 6.5 m diameter refers to the largest possible flat-to-flat diameters at any azimuthal angle, not the average ($\sim$5.9 m) or minimal one ($\sim$5.3 m), appropriate for evaluation of its resolving power. The 25 m^2 clear aperture would be representative for a round 6.06 m mirror (assuming obscuration by 0.2 m wide support beams and a 0.5625 m diameter central hole).

Table 1. JWST primary mirror assembly: diameters

Option	$N_{\rm hex}$	$A_{\rm clear}$ [m^2]	"D" [m]	D_{θ_1} [m]	$D_{\rm A}$ [m]	$D_{\rm min}$ [m]
reference	$\cdots$	34.0	7.0	7.00	7.00	7.00
0	36	29.4	7.0	6.40	6.54	5.80
3	36	25.0	6.5	5.90	6.07	5.34
4	18	25.0	6.6	6.05	6.07	5.50
1B	36	22.7	6.2	5.65	5.80	5.10
2B	18	22.7	6.3	5.75	5.80	5.20

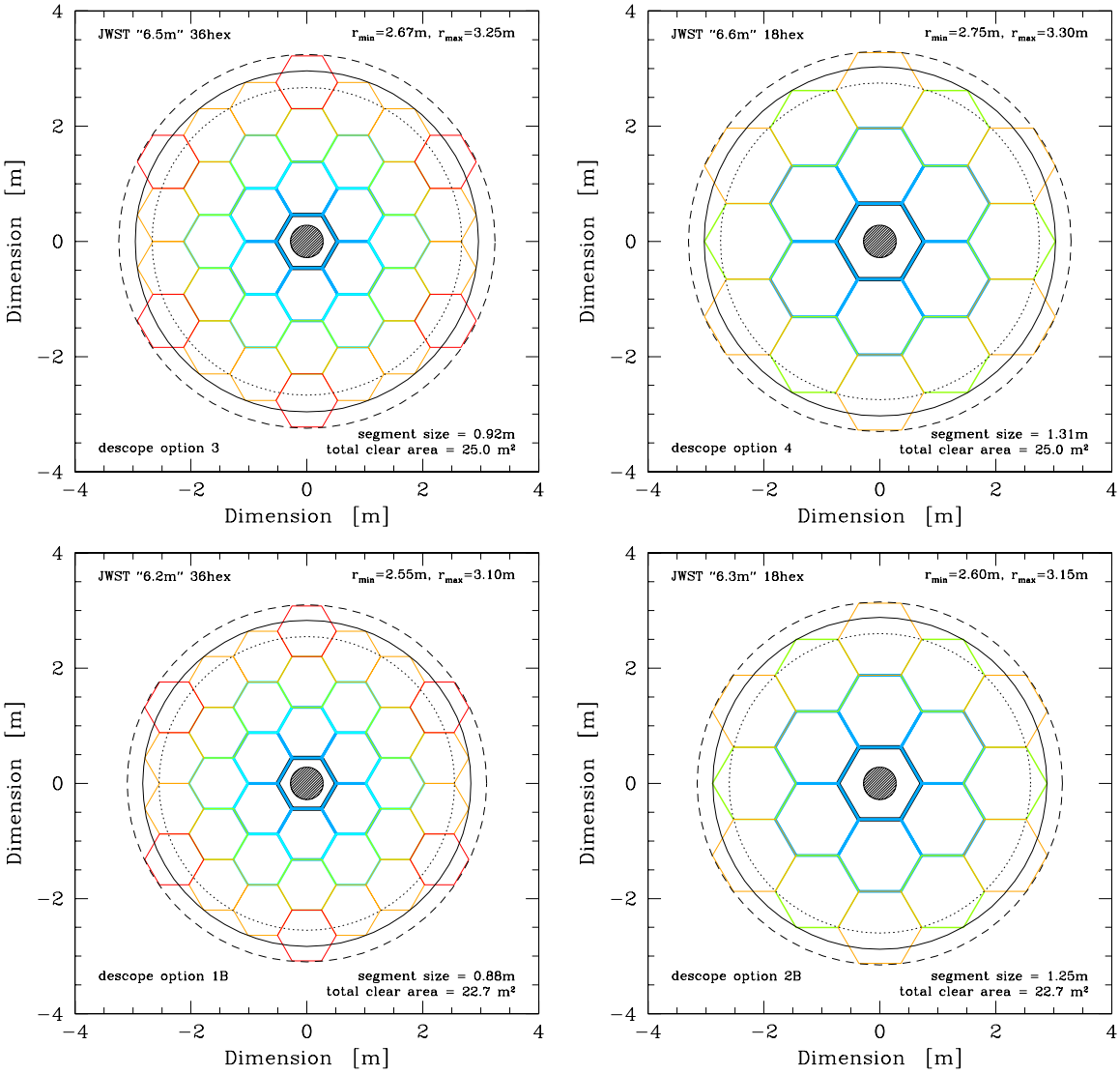

FIG.1 — Graphical representations of the 36- and 18-segment primary mirror assemblies under study. Overlayed on the segmented mirror are three circles corresponding to the minimim, average and maximum diameter reached at any azimuthal angle. In the following, we use the average diameter for evaluation of the resolution of JWST.

3. Point Spread Functions

Ball Aerospace provided us for this study with ray-traced PSF shapes for the 6 configurations of the primary mirror assembly corresponding to the "baseline" 7.0 m configuration, and to descope options "1B" (6.2 m/22.7 m^2, 36 segments), and "2B" (6.3 m/22.7 m^2, 18 segments), each both for a tip/tilt/piston (3 DoF) and for a hexapod (6 DoF) mirror support and actuation system. We assume the PSF shapes for descope options "3" (6.5 m/25.0 m^2, 36 segments) and "4" (6.6 m/25.0 m^2, 18 segments) to closely resemble those for options "1B" and "2B".

For each configuration, 10 Monte Carlo realizations of the total PSF were provided for

four different wavelengths (0.7, 2.0, 10, and 20μm), each sampled on a 256×256 regular grid. The PSF's were converted to FITS format PSF-images and average PSF's were generated for each of the configurations and for each wavelength, rejecting the two lowest and two highest values in each stack of 10 pixels.

Synthetic aperture photometry was performed on each of the averaged PSF's, and radial response curves were constructed. The criterion that JWST be diffraction limited at $\lambda \geq 2\mu$m gives us the absolute angular scale of each of the PSF's, via the radius (angle) of the first Airy minimum:

$$\theta_1 = 1.22 \cdot (\lambda/D) \quad (1)$$

where for D we take the azimutal average diameter rather than the maximum flat-to-flat diameter. For observations at 0.7μm, we substitute 2.0μm for λ, since JWST will not be diffraction limited shortward of $\sim$2μm. Table 2 lists the PSF pixel scales and NIRCAM pixel scale as used in the simulations below. Figs. 2–4 show greyscale renditions of the PSF's and derived radial response and enclosed energy profiles at 0.7, 2.0, and 10μm.

For the purpose of convolving these PSF's with the observed Hubble Deep Field (Williams et al. 1996) F814W image, we must account for the HST PSF. In F814W, $\theta_1^{HST} = 1.22 \cdot (0.814 \times 10^{-6}/2.4) = 0.085''$, so straight convolution with the JWST PSF would yield an effective resolution $\sqrt{0.085^2 + (1.22\,(2.0 \times 10^{-6}/[\text{“6.2”} - \text{“7.0”}]))^2} \sim [0''.117 - 0''.111]$, i.e., $\sim$1.4× too large. So for the purpose of convolution we need to assume a PSF pixel scale that is smaller than the actual pixel scale by the same factor. We adopt the following relative pixel scales:

```
At 0.7 micron: 3.4412 PSF pixels/image pixel for the 7.0, 6.5 and 6.2 m
                      (36 hex) mirror designs
               4.7028 PSF pixels/image pixel for the 6.6 and 6.3 m (18 hex);
At 2.0 micron: 3.2297 PSF pixels/image pixel for the 7.0, 6.5 and 6.2 m
                      (36 hex) mirror designs
               4.2248 PSF pixels/image pixel for the 6.6 and 6.3 m (18 hex).
```

In order to construct a convolution kernel, PSF's need to be generated with pixel sizes that fit an integer number of times in a NIRCAM image pixel. Since we will subsample the HDF F814W image by drizzling it onto pixels that are $\frac{1}{3}$ the size of the JWST/NIRCAM pixels, we need to match the PSF pixels to that size. This procedure mitigates the effects of the imprint of the HST PSF and simulates as best we can performing the convolution prior to the sampling onto the discrete NIRCAM pixels, while keeping almost the full resolution in the JWST PSF's.

```
At 0.7 micron: 7.0, 6.5 and 6.2 m --> magnify PSF pix by 3/3.4412 = 0.87179
               6.6 and 6.3 m      --> magnify PSF pix by 3/4.7028 = 0.63792
At 2.0 micron: 7.0, 6.5 and 6.2 m --> magnify PSF pix by 3/3.2297 = 0.92888
               6.6 and 6.3 m      --> magnify PSF pix by 3/4.2248 = 0.71009
```

Appendix A lists an example of a script used to perform the convolution of a 2048×2048 pixel portion of the version-2 F814W drizzled HDF-N with a JWST PSF.

Table 2. Adopted PSF and NIRCAM pixel scales

Option	$N_{\rm hex}$	"D" [m]	λ [μm]	θ_1 [pix]	$\theta_1^{a,b}$ [$''$]	$\psi_{\rm PSF}$ [$''$/pix]	$\psi_{\rm NIRCAM}{}^{c}$ [$''$/pix]
0	36	7.0	0.7	4.39	0.078638	0.017913	0.04222
0	36	7.0	2.0	4.12	0.078638	0.019087	0.04222
3	36	6.5	0.7	...	0.085303	0.019431	0.04580
3	36	6.5	2.0	...	0.085303	0.020705	0.04580
4	18	6.6	0.7	...	0.083188	0.013865	0.04466
4	18	6.6	2.0	...	0.083188	0.015434	0.04466
1B	36	6.2	0.7	4.39	0.089077	0.020291	0.04783
1B	36	6.2	2.0	4.12	0.089077	0.021621	0.04783
2B	18	6.3	0.7	6.00	0.087528	0.014588	0.04699
2B	18	6.3	2.0	5.39	0.087528	0.016239	0.04699

Note. — *a*) The listed PSF pixel scales for Options "3" and "4" where scaled from those for Options "1B" and "2B"; *b*) we adopt the azimuthal average mirror diameter for D; *c*) the short-wavelength channel of NIRCAM is assumed to have 3.725 pixels per FWHM at 2.0μm for a point source.

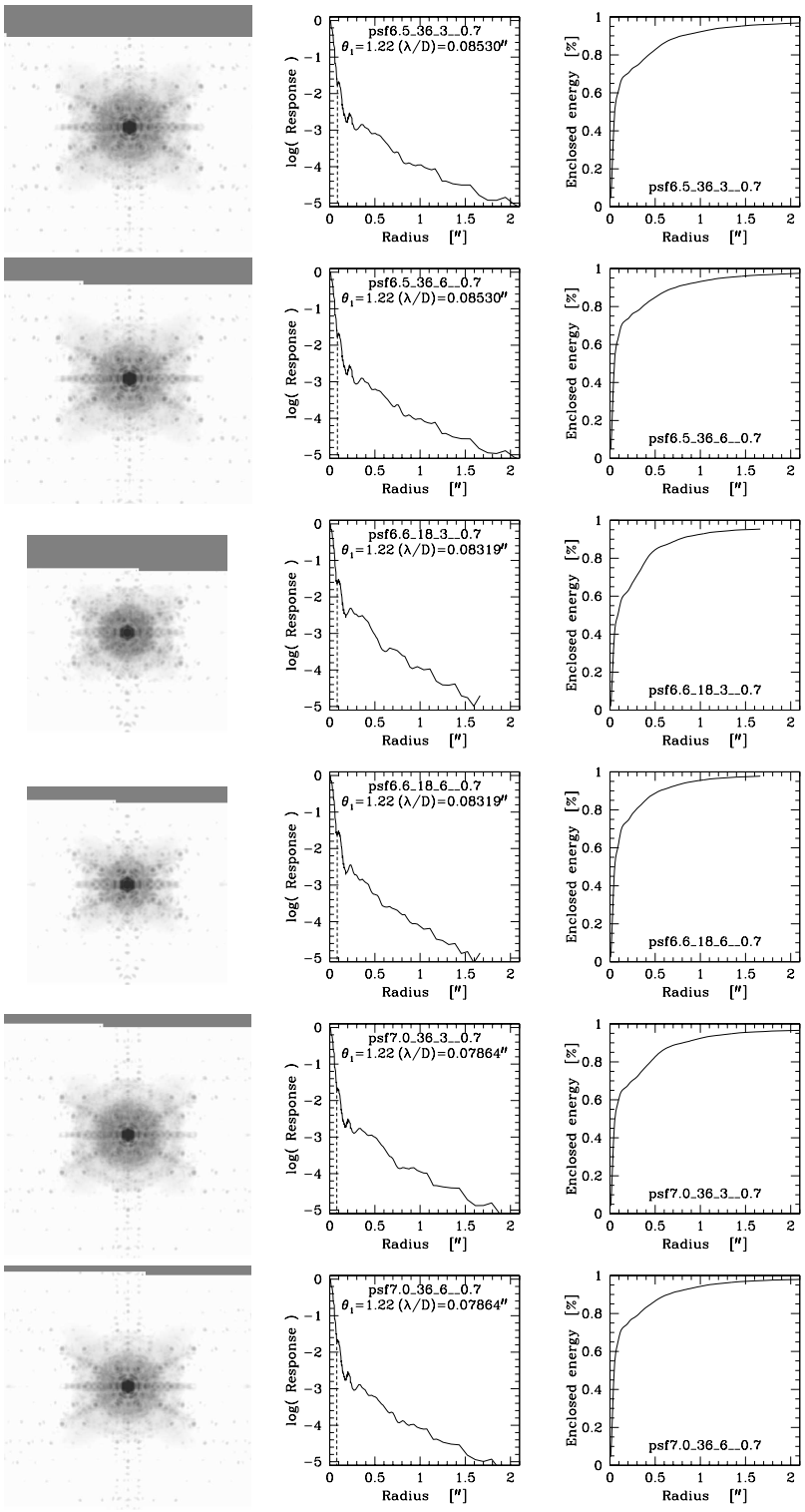

FIG.2 — Greyscale renditions, radial intensity and enclosed flux profiles of the average of 10 Monte Carlo simulations at λ=0.7μm for six different JWST mirror configurations [courtesy A.A. Barto, Ball Aerospace]. Each image has the same scale and is displayed using the same logarithmic stretch. From top to bottom: a 36-hex 6.5 m primary with tip/tilt/piston (3 DoF) and one with hexapod (6 DoF) support and actuation; a 18-hex 6.6 m primary with 3 DoF, and one with 6 DoF; a 36-hex 7.0 m primary with 3 DoF, and one with 6 DoF. The 6 DoF configuration is preferred, since it reduces the amount of flux in the PSF halo at $\lambda \lesssim 1\mu$m.

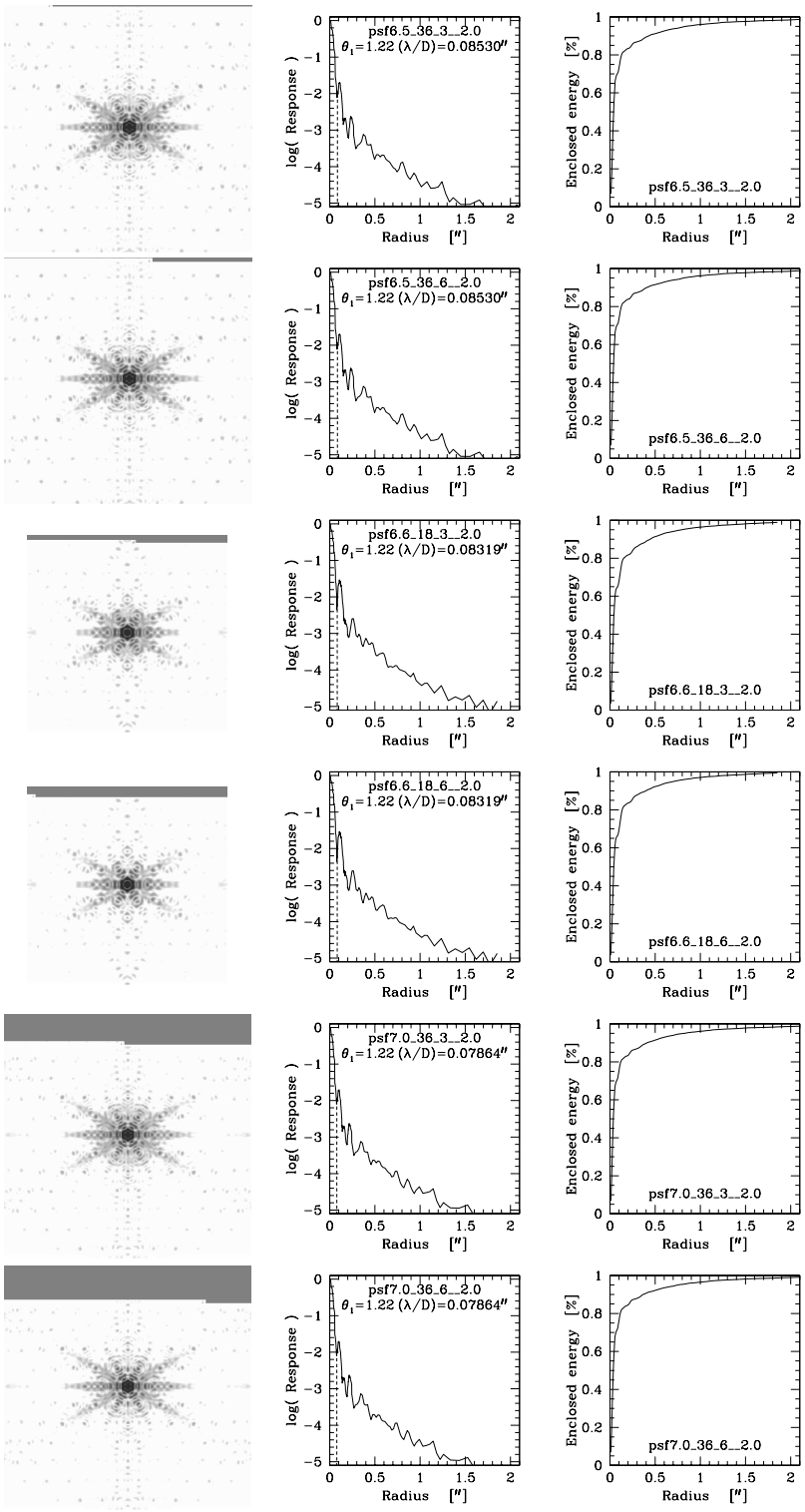

FIG.3 — As Fig. 1 for λ=2.0μm.

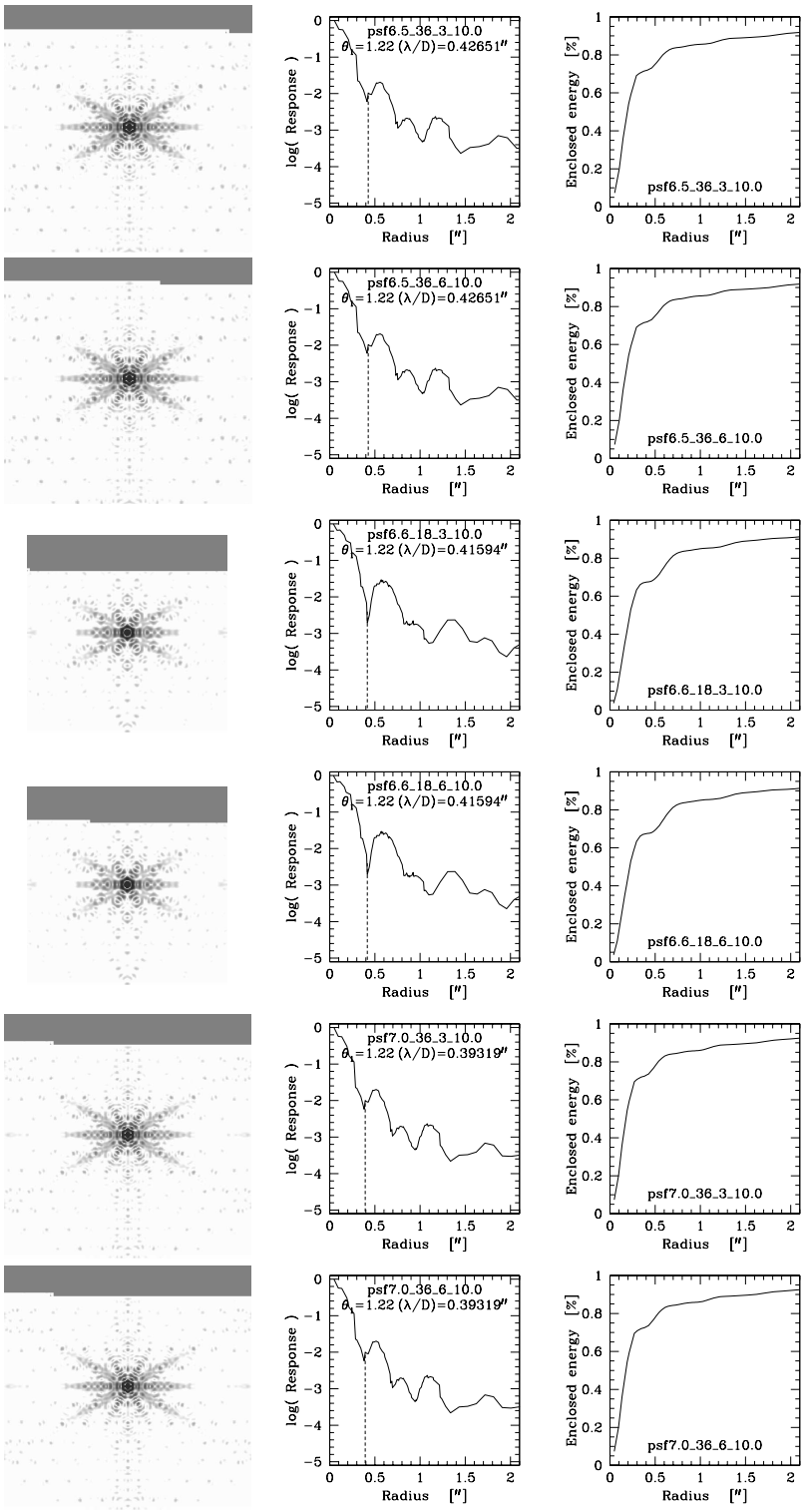

FIG.4 — As Fig. 1 for λ=10.0μm.

Figures 5 through 8 show four examples of the resulting simulated JWST images at 0.7μm. Since convolving an observed image with a PSF smoothes the noise present in that image to some degree, we added back in random noise such that the rms of a black region of sky again matches that in the original image.

We subsequently detected and measured objects in each simulated JWST image using `SExtractor v2.2.2` (Bertin & Arnouts 1996). We will focus on the effective radii, axis ratios, and position angle measurements, as well as object magnitudes. Object lists for different simulations were matched against one another, taking into account the difference in image scale, and the results are plotted in Figures 9 through 11 for 0.7μm.

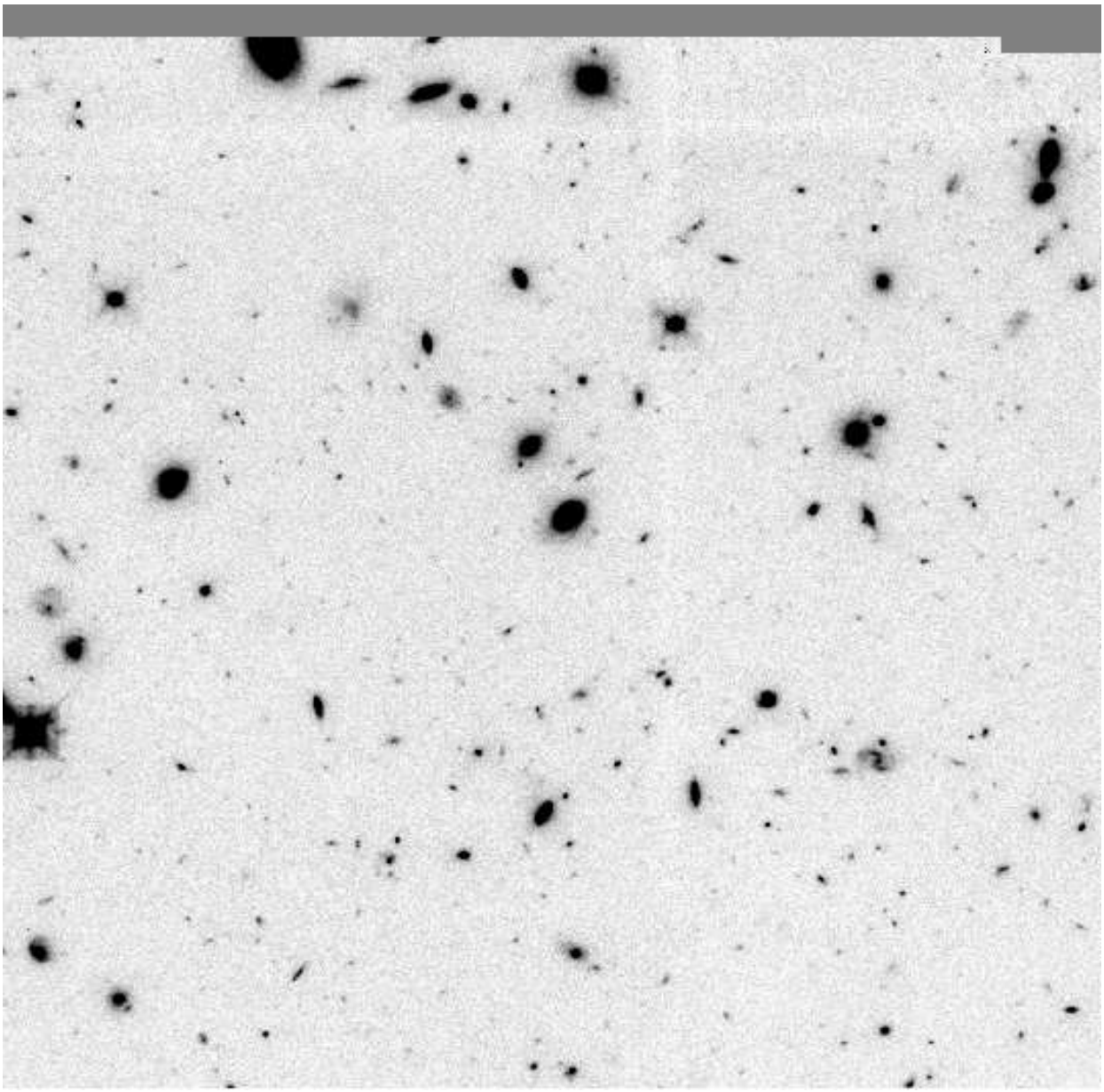

FIG.5 — Simulated JWST deep field at 0.7μm for a 7.0 m flat-to-flat, 36-segment primary mirror design and hexapod mirror actuation. The above image is based on a 2048×2048 portion of the 50-orbit HDF-N F814W mosaic.

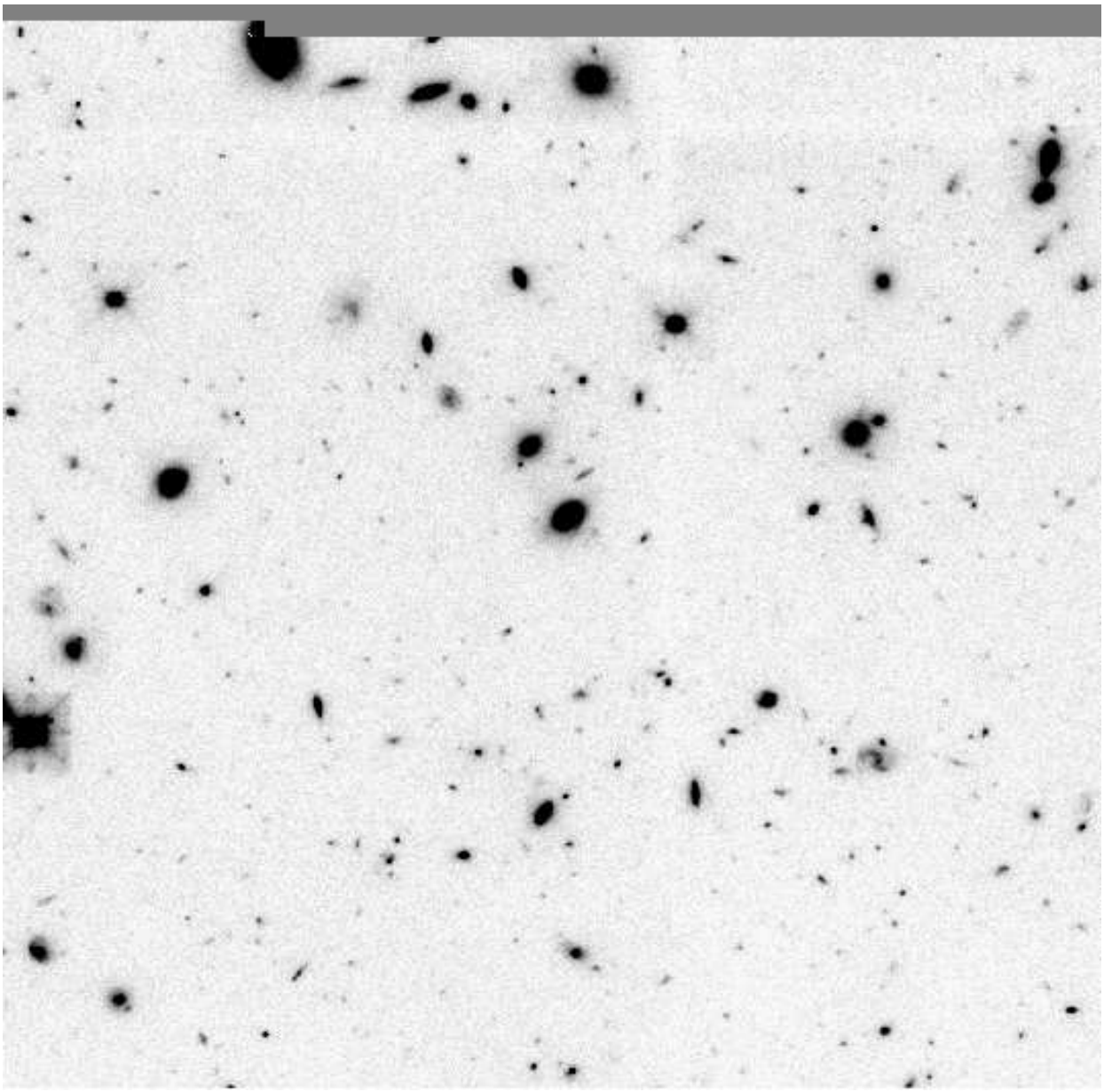

FIG.6 — As Fig. 5 for a descoped 25 m^2 clear aperture JWST with a 6.6 m flat-to-flat, 18-segment primary mirror design and hexapod mirror actuation.

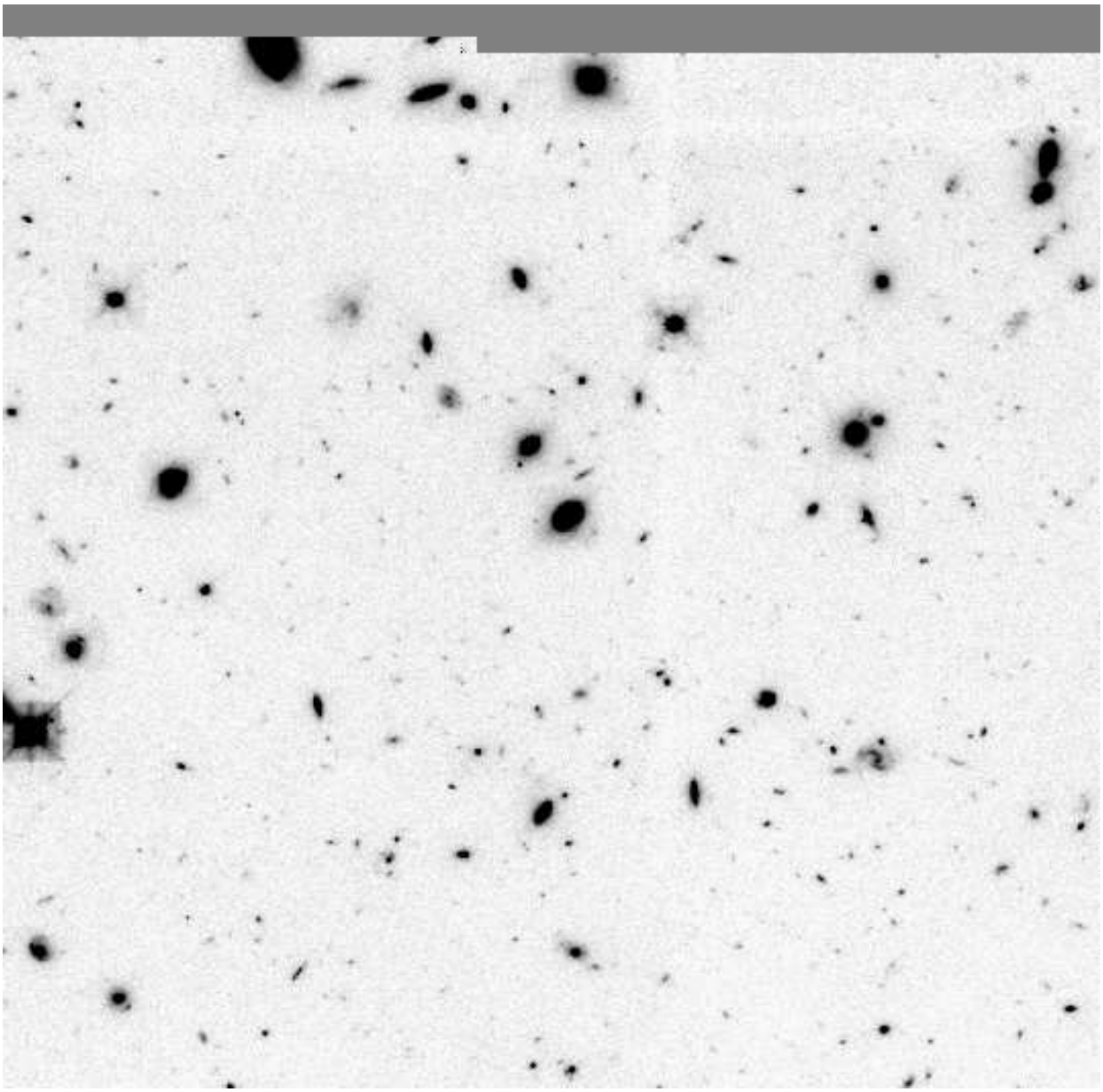

FIG.7 — As Fig. 5 for a descoped 25 m^2 clear aperture JWST with a 6.5 m flat-to-flat, 36-segment primary mirror design and hexapod mirror actuation.

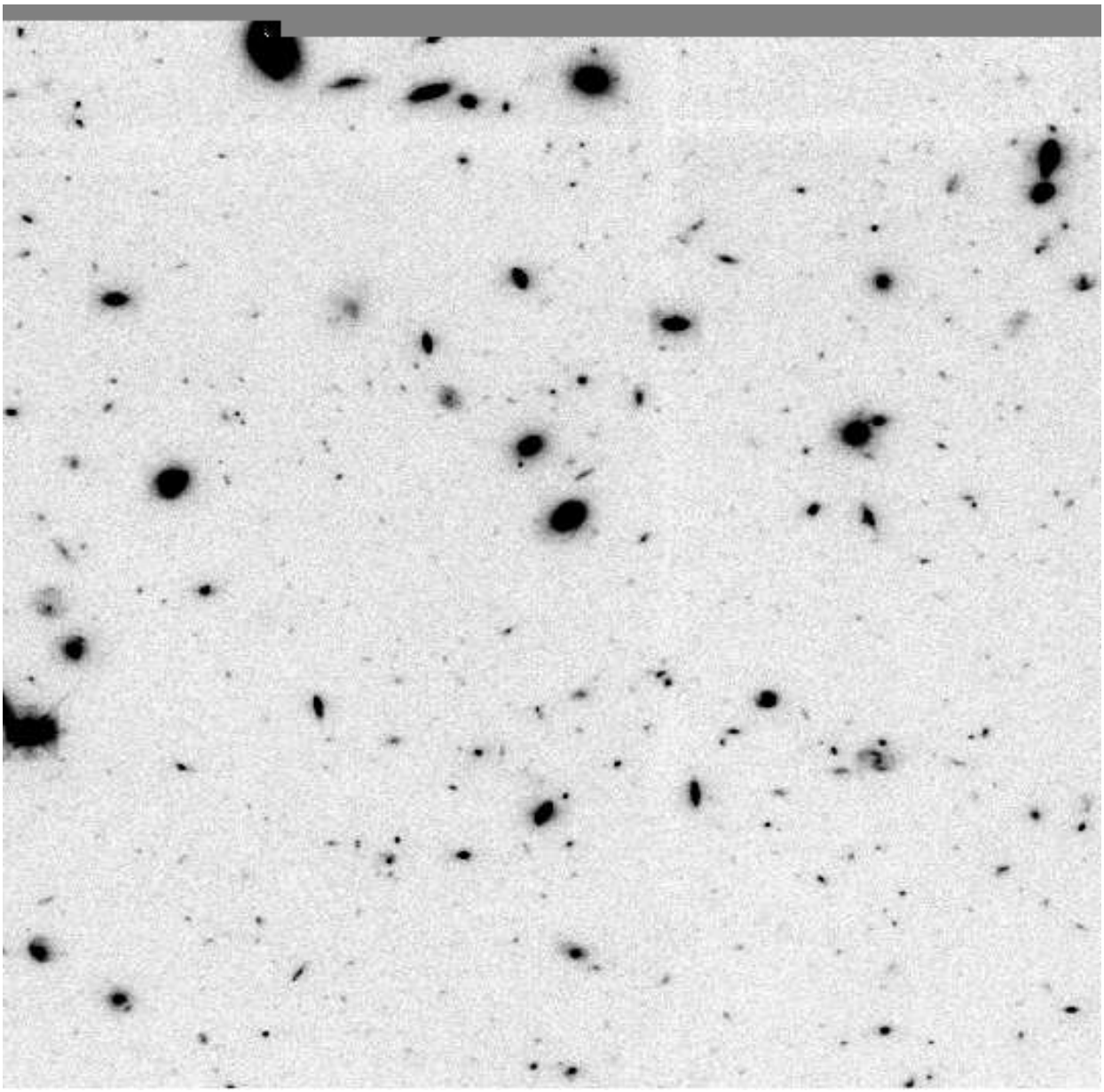

FIG.8 — As Fig. 5 for a descoped JWST with a non-circular 7.0×3.5 m aperture.

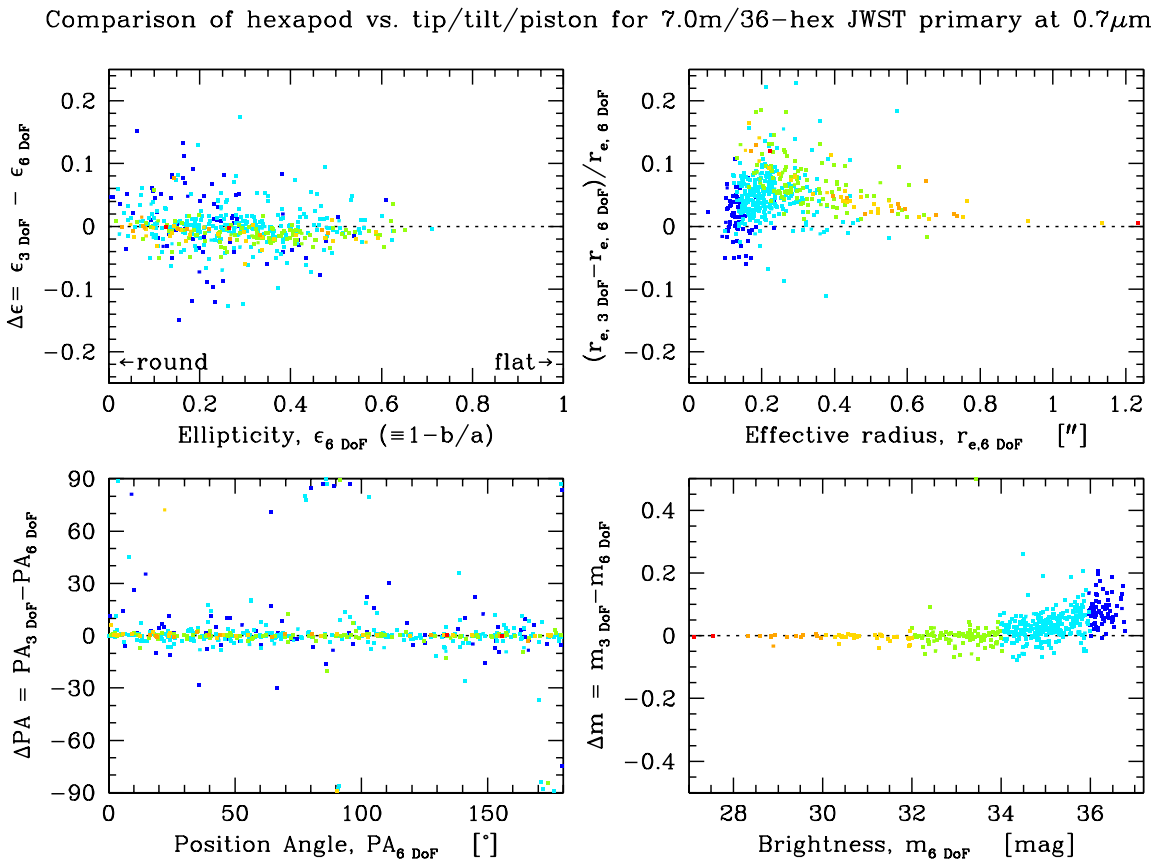

FIG. 9 — Comparison of object parameters recovered from simulations at 0.7μm for a 7.0 m JWST primary mirror assembly with tip/tilt/piston (3 DoF) mirror support and actuation versus one with hexapod (6 DoF) actuation [see Fig. 5]. Points are color-coded according to their apparent brightness. Hexapod actuation performs better in retrieving the effective radii of small objects ($0\farcs2 \lesssim r_e \lesssim 0\farcs6$) and results in a smaller percentage of the object flux scattered to large radii. There is also a marginally better performance in retrieving the axis ratios of flattened systems. Note that the SExtractor (Bertin & Arnouts 1996) magnitudes shown have an arbitrary zeropoint.

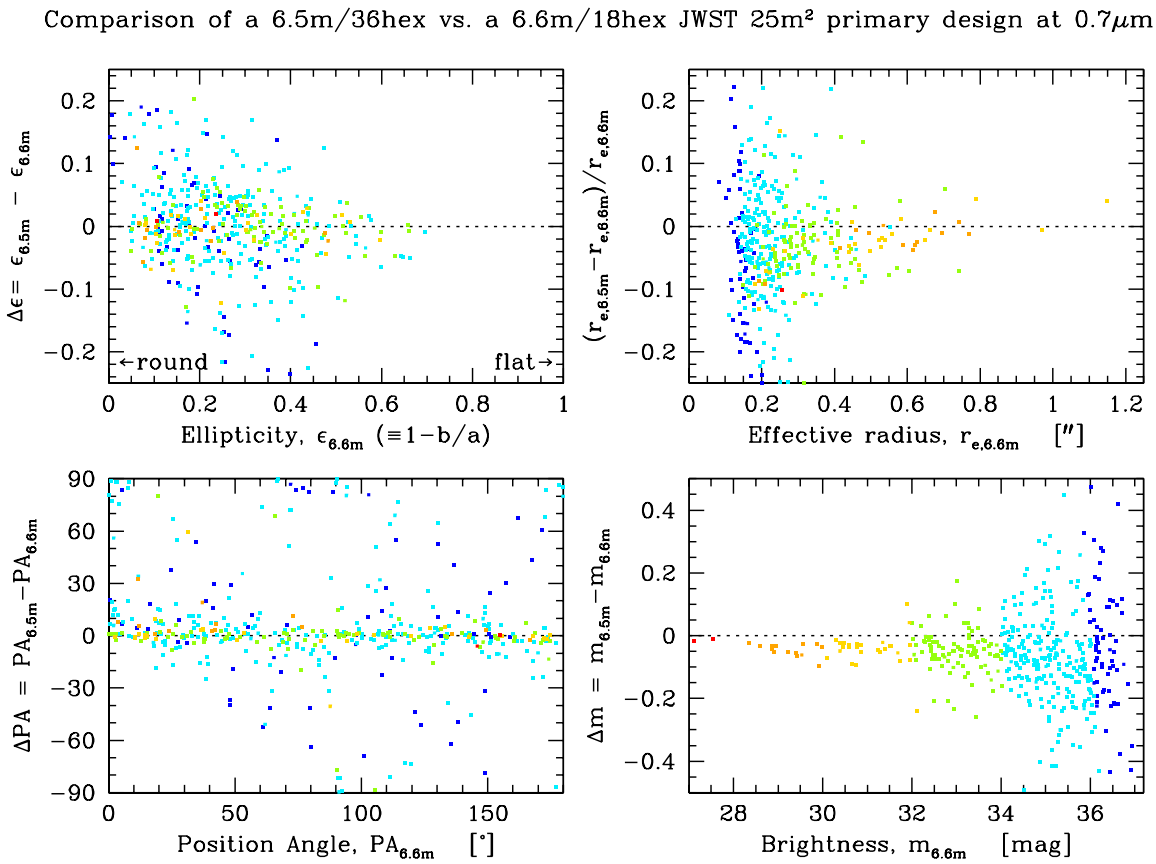

FIG.10 — Comparison of object parameters recovered from simulations at 0.7μm for a 18-segment and a 36-segment primary mirror assembly, both giving a 25 m^2 clear aperture and both having hexapod mirror actuation.

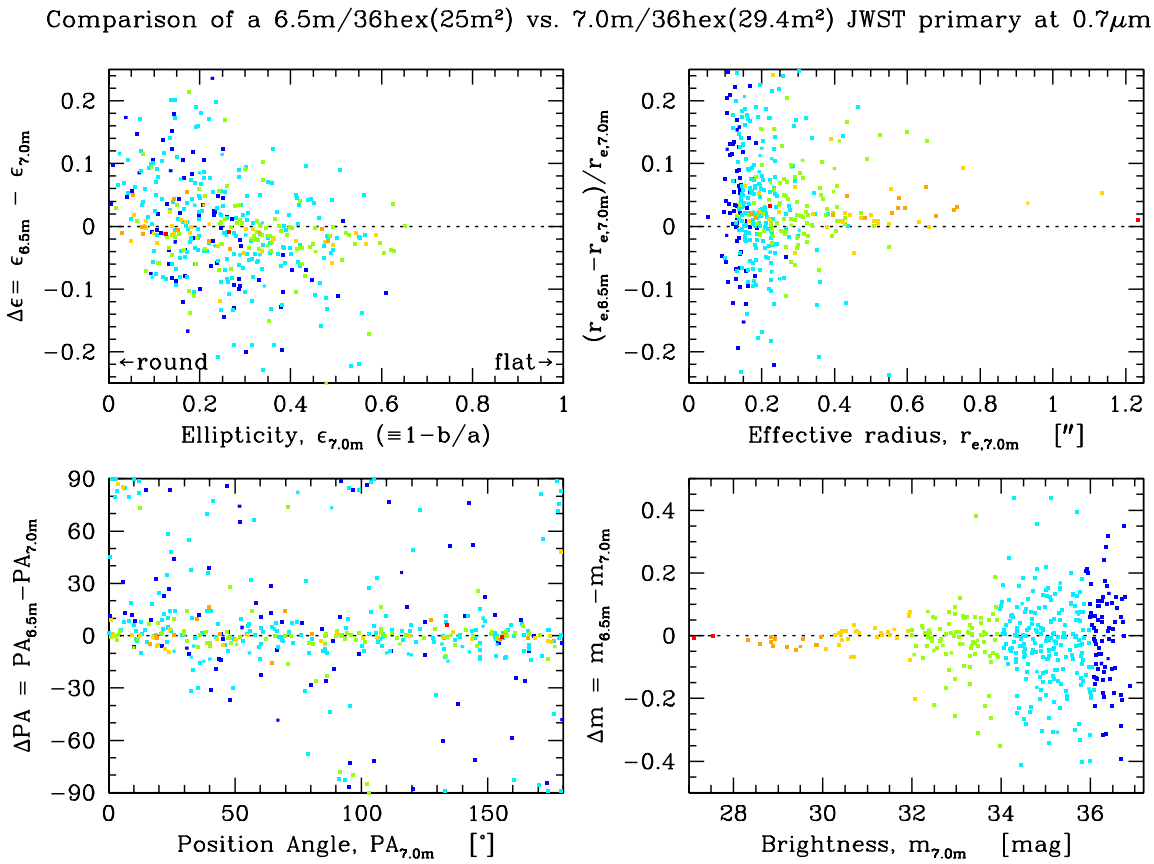

FIG.11 — Comparison of object parameters recovered from simulations at 0.7μm for a 36-segment 7.0 m flat-to-flat (29.4 m^2 clear aperture) primary mirror and for a descoped 6.5 m (25 m^2) mirror of the same design, both having hexapod mirror actuation.

RAJ and RAW acknowledge support from NASA grant NAG5-12460 for the work presented in this report. We thank Seth Cohen and Stephen Odewahn for help with LMORPHO.

REFERENCES

Bertin, E., & Arnouts, S. 1996, A&AS, 117, 393

Williams, R.E., Blacker, B., Dickinson, M., et al. 1996, AJ, 112, 1335

Appendix A

Below, we list the transcript of an IRAF script used to perform the convolution of a 2048×2048 pixel portion of the HDF-N (F814W) with the JWST for a 7.0 m 36-segment primary mirror assembly and hexapod mirror actuation for a wavelength of 0.7μm. The native resolution of the HDF mosaic is $0''.03983$/pix and the HDF image is subsampled by drizzling onto a grid of pixels that are $\frac{1}{3}$ the NIRCAM pixel size assumed for this mirror configuration ($0''.04222$/pix). The JWST PSF is slightly subsampled to match.

```
gdate()
print ("PSFMCONV: psf7.0_36_6__0.7                          "//gdate.adate)
print ("  DRIZ_HDF2JWST: f814_mos2048.fits  oldpix=0.03983\" --> newpix=0.04222/3\" ...")
drizzle ("f814_mos2048.fits", "f814_mos2048d.fits", outweig="", in_mask="",
  wt_scl="exptime", pixfrac=0.65, scale=real(0.04222/0.03983/3), coeffs="",
  outnx=int(1.+3*2048*0.03983/0.04222), outny=int(1.+3*2048*0.03983/0.04222),
  lambda=814., xsh=0., ysh=0., rot=0., shft_un="input", shft_fr="input",
  align="center", expkey="exptime", in_un="cps", out_un="cps",
  fillval="INDEF", >> "/dev/null")

print ("  DRIZ_PSF2PSF: psf7.0_36_6__0.7.fits  0.01791309\" --> "//real(0.87179*0.04222/3)//"\" ...")
hedit ("FITS/psf7.0_36_6__0.7.fits", "exptime", "1.00", add+, delete-,
  verify-, show-, update+)
drizzle ("FITS/psf7.0_36_6__0.7.fits", "psf7.0_36_6__0.7d.fits", outweig="",
  in_mask="", wt_scl="exptime", pixfrac=0.65, scale=real(0.87179),
  coeffs="", outnx=int(1.+256/0.87179), outny=int(1.+256/0.87179),
  lambda=814., xsh=0., ysh=0., rot=0., shft_un="input", shft_fr="input",
  align="center", expkey="exptime", in_un="cps", out_un="cps",
  fillval="INDEF", >> "/dev/null")
imgstat ("psf7.0_36_6__0.7d.fits", verbose=no)
imarith ("psf7.0_36_6__0.7d.fits", "/", imgstat.sum, "psf7.0_36_6__0.7d.fits",
  hparams="", pixtype="real", calctype="real", verbose=no, noact=no)

print ("  MKPSFKERN: psf7.0_36_6__0.7d.fits --> \"psf7.0_36_6__0.7d.kern\" ...")
imgets ("psf7.0_36_6__0.7d.fits", "naxis1")
imgets ("psf7.0_36_6__0.7d.fits", "naxis1")
vstor (cval2=imgets.value)
listpix ("psf7.0_36_6__0.7d.fits", formats="%5d %5d %12.7f\n",
  wcs="logical", verbose=no, > "tmp.kern")
iwc ("tmp.kern")
print ("#!/bin/csh", > "tmpmkkrn")
print ("splitany tmp.kern `range -n "//vstor.cval2//" "//vstor.cval2//" - "//str(iwc.nlines)//"`",>>"tmpmkkrn")
print ("set i = 0", >> "tmpmkkrn")
print ("while ( $i < "//vstor.cval2//" )", >> "tmpmkkrn")
print ("    @ i = $i + 1", >> "tmpmkkrn")
print ("    awk '{print $3}' tmp.kern.$i >> psf7.0_36_6__0.7d.kern", >> "tmpmkkrn")
print ("    echo ';' >> psf7.0_36_6__0.7d.kern", >> "tmpmkkrn")
print ("    \\rm -fr tmp.kern.$i", >> "tmpmkkrn")
print ("end", >> "tmpmkkrn")
!chmod 700 tmpmkkrn
!tmpmkkrn
delete ("tmp.kern,tmpmkkrn")

vstor(cval1=str(int(1.+3*2048*0.03983/0.04222)))
vstor(rval1=0.1*int(10*(12*(real(imgets.value)*int(1.+3*2048*0.03983/0.04222))**2/1740.e6/3600.))
print ("  PSFCONVOLVE: f814_mos2048d["//vstor.cval1//","//vstor.cval1//"]*\
                                                  psf7.0_36_6__0.7d["//vstor.cval2//","//vstor.cval2//"]")
convolve ("f814_mos2048d.fits", "tmpf814_mos2048d.fits",
  "psf7.0_36_6__0.7d.kern", bilinear=no, radsym=no, boundary="nearest",
  constant=0., row_del=";")
drizzle ("tmpf814_mos2048d.fits", "f814_mos_7.0_36_6__0.7.fits", outweig="", in_mask="",
  wt_scl="exptime", pixfrac=0.65, scale=3., coeffs="",
  outnx=int((1.+3*2048*0.03983/0.04222)/3), outny=int((1.+3*2048*0.03983/0.04222)/3),
  lambda=814., xsh=0., ysh=0., rot=0., shft_un="input", shft_fr="input",
  align="center", expkey="exptime", in_un="cps", out_un="cps",
```

```
  fillval="INDEF", >> "/dev/null")
sleep 5
imdelete ("tmpf814_mos2048d.fits,f814_mos2048d.fits", yes, verify=no,
  default_acti=yes)

gdate()
print ("PSFMCONV: Finished at "//gdate.adate)
printf("\n", >> "psfmconv.log")
```